Global View of Engineering Geology and the Environment – Wu & Qi (eds)
© 2013 Taylor & Francis Group, London, ISBN 978-1-138-00078-0

Centrifugal experiment on stratum instability and failure process due to gas hydrate dissociation

Xiaobing Lu & Xuhui Zhang
Institute of Mechanics, Chinese Academy of Sciences, Beijing

Guanghai Hu
The First Institute of Oceanography, SOA, Qingdao

ABSTRACT: Centrifugal experiments were carried out to investigate the stratum instability caused by the dissociation of gas hydrate. First gas hydrate-bearing sample was synthesized using biological anaerobic fermentation method. The silty sand was taken as the skeleton. Then four centrifugal experiments were carried out to study the responses of stratum to the dissociation of the gas hydrate. The characteristics of stratum slide and pore pressure variation and displacement were observed. It is shown that the produced gas can cause the increase of pore pressure and slope slide towards the toe during and after dissociation of gas hydrate. The failure occurs first at the toe of the sample and slides downwards along an arc sliding face. Cracks form at the top of the slope. The slope angle becomes smaller and smaller. This work is beneficial to the further study on the instability conditions of stratum due to the dissociation of gas hydrate.

Keywords: methane gas hydrate, centrifugal experiments, stratum stability, failure process

1 INTRODUCTION

Natural Gas Hydrate (NGH) is a new potential source of energy in the world. Many researchers study the exploitation and exploration of NGH recently. Most of previous attentions are paid on the exploitation of NGH (Sakamoto et al., 2007, 2009). However, NGH dissociation can decrease the strength of NGH sediment and induce kinds of hazards such as stratum landslide (Lu et al., 2008, 2010, 2011; Zhang et al., 2011; William et al., 2004). For example, the Storegga slide in Norway (Locat and Lee, 2002; Hovland et al., 2001), Cape Fear slide in east coast of America and the landslide in continental shelf of west Africa (Kayer and Lee, 1991; Sultan et al., 2004) and some other landslides (Gilles et al., 1999) in oceans all resulted from NGH dissociation. Thus it is very important to know if the NGH-bearing sediment and its structures are stable during/after dissociation of NGH. However, only few analyses on the stratum instability resulted from NGH dissociation have been carried out.

In this paper, the development of deformation and pore pressure in NGH stratum were investigated by centrifugal experiments. These results were beneficial to the understanding of stratum instability due to the dissociation of gas hydrate.

2 INTRODUCTION OF EXPERIMENTS

2.1 *Experimental apparatus*

The experiments were performed in the 450 g-ton centrifuge in China Institute of Water Resources and Hydropower. The maximum centrifugal acceleration is 300 g. The size of the hanging basket is length × width × height = 1.5 m × 1.0 m × 1.2 m. The maximum gyration radius is 5.03 m. The inner size of the model tank used in experiments is length × width × height = 0.54 m × 0.4 m × 0.4 m (Fig. 1). Three samples were prepared with slope angles of 7.1, 8, 10 degrees respectively. Six PDCR-81 type

Figure 1. Low temperature box and high pressure tank.

PPTs (Pore Pressure Transducer), made in US, were buried in the sediment to measure the pore pressure. Two sets of digital cameras were used to record the change of sediment's surface during dissociation of gas hydrate. Three laser displacement transducers (LS1, LS2 and LS3) were located over the samples with distances of 5 cm, 25 cm and 45 cm to the top of slopes respectively and all with a distance to one side wall 20 cm.

The sample was synthesized in a high pressure tank (the maximum permissible pressure is 5 MPa) with a height of 1.45 m and net diameter of 0.9 m (Fig. 1). The lowest temperature was −16°C. The specific gravity of the silty sand used to format hydrate-bearing sediment was 2.71. The grain series curve is shown in Figure 2. Figure 3 shows the whole gas hydrate-bearing sample (after dissociation).

2.2 *Experimental conditions*

Some organic matter was mixed with the soil in a model tank with a size of $60 \times 35 \times 35$ cm^3 to form methane distributed uniformly in the soil. After about 4 days, the model tank was moved into a tank which can provide high pressure to form gas Hydrate-Bearing Sediment (HBS) under a pressure of 4 MP and temperature of −14°C and this state was kept for two days. The depths of PPTs in the sediment are shown in Table 1. The physical and geometrical parameters are shown in Table 2.

Three cases were adopted in experiments:

Case 1: The skeleton of the sample is fully consisted of silty sand. During 0–2850 s, the centrifugal acceleration increased from 0 to 150 g gradually and then this state was kept for 3000 s.

Case 2: A 10 mm thick clay layer covered the HBS. During 0–2670 s, the centrifugal acceleration increased from 0 to 150 g gradually and then this state was kept for 840 s.

Case 3: A heater was placed near PPT1 and began to work once the centrifuge was started. During 0–600 s, the centrifugal acceleration increased from 0 to 150 g gradually and this state was kept for 3600 s.

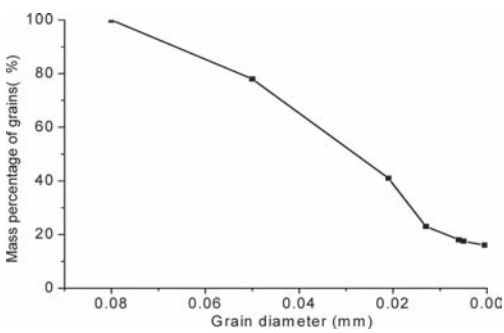

Figure 2. Grain series of the soil.

Figure 3. Soil surface of soil layer after anaerobic fermentation (the holes are formed by CH4 drainage).

2.3 *Displacement of sample*

With the increase of the gravity acceleration, sediment settles gradually to a stable value. After stop of centrifuge, the development of settlement and pore pressure continue for a while. The settlement at the top of the slope is larger than that at the toe in all the three cases. In the third case, the settlement increases at later stage because the soil at the top slides downwards. The failure occurs first at the toe of the sample and slides downwards along an arc sliding face. Cracks form at the top of the slope. In case 1, the slope becomes stable again at the slope angle of 6.7° (Fig. 4). In case 2, the final

Table 1. Depth of PPTs.

No.	1	2	3	4	5	6
Case 1	10.5	9	12	9.5	18.3	17.3
Case 2	28.1	9.8	14	9	10.4	2
Case 3	15.5	7.3	13.5	24.9	10.9	10.9

Note: Numbers 1~6 in line 1 denote PPT1~PPT6.

Table 2. Initial parameters of the sample.

Parameter	Case 1	Case 2	Case 3
S_w (%)	33.0	33.9	34.1
ρ (g/cm^3)	1.84	1.83	1.81
S_c (mmol/kg)	1.2	1.1	1.3
θ (°)	7.1	8.5	10

Note: S_w denotes water content, ρ denotes density, S_c denotes CH4 content, θ denotes slope.

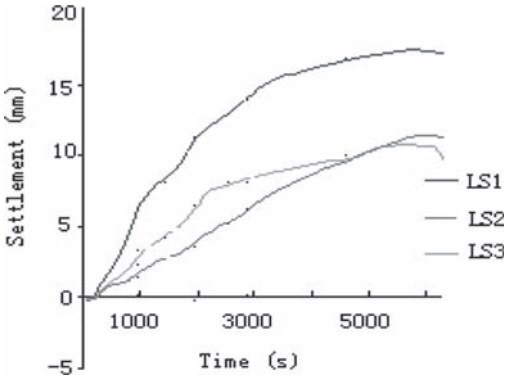

Figure 4. Development of settlement in case 1.

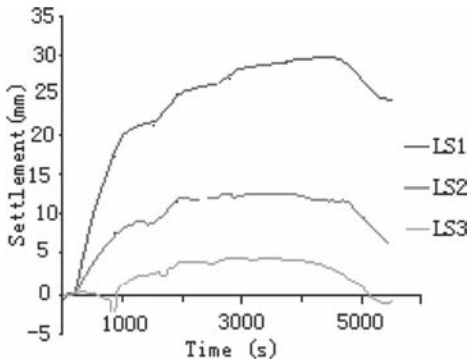

Figure 5. Development of settlement in case 2.

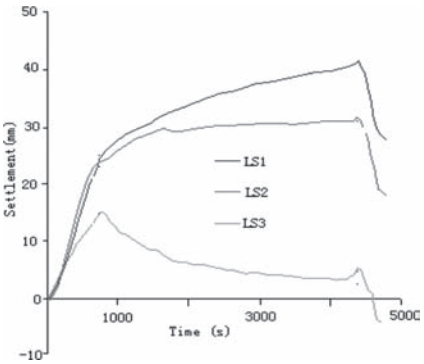

Figure 6. Development of settlement in case 3.

stable slope angle is 5.1° (Fig. 5). The maximum settlements at LS1 and LS2 are 29.6 mm and 13.0 mm, respectively. The final stable slope angle is 4.2° in case 3 (Fig. 6). The slope angle was determined by measurement of the height relative to the bottom of the box and horizontal position relative to the toe of the slope of some points at the surface.

2.4 *Development of pore pressure*

The development of pore pressure recorded by PPT1, PPT3~PPT6 in case 1 are shown in Figure 7. The data recorded by PPT2 are not adopted because they are obviously mistaken. The pore pressure recorded by each PPT increases with the centrifugal acceleration from 0 to 150 g. The sequence of the PPTs by the start point that the pore pressure rises is PPT6, PPT5, PPT4, PPT3 and PPT1, which means, that the pore pressure increases first near the boundaries of the model tank because the gas hydrate at these positions dissociates first (Fig. 8). In case 2, the pore pressures recorded by PPT1, PPT3, PPT5, PPT4 and PPT6 are 68.5 KPa, 123.7 KPa, 152.8 KPa, 176.2 KPa and 373.4 KPa respectively when the centrifugal acceleration increases to 150 g. The pore pressures decrease when the acceleration is kept for 50 g, 100 g and 150 g respectively for some time (Fig. 9) due to the dissipation of the pore pressure. In case 3, the pore pressure recorded by PPT4 is linearly proportional to the centrifugal acceleration because it is located in clean water. The data recoded by PPT4 can be used to certificate the reliability of the transducer and compared with that recorded by other PPTs. The recorded data

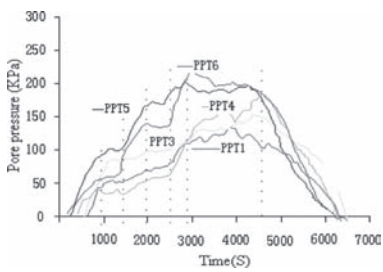

Figure 7. Development of pore pressure in case 1.

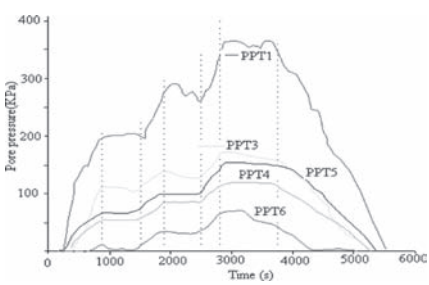

Figure 8. Development of pore pressure in case 2.

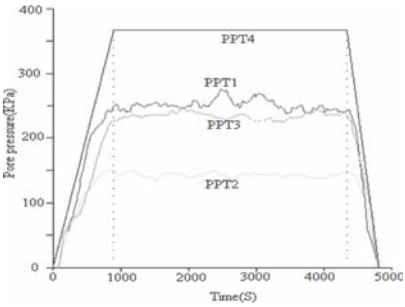

Figure 9. Development of pore pressure in case 3.

of PPT1, PPT2 and PPT3 at 150 g are 249.6 KPa, 150.7 KPa and 225.3 KPa, respectively. The wave of data at the state of 150 g means the pore pressure is being generated and dissipated.

From the above results, it can be seen that if there is an over layer with low permeability or is dissociated faster (such as by heating), the settlement and pore pressure become larger than that without such a cover layer and dissociating slowly. The pore pressure at the upper part and near the sidewall increases faster than that at the rest part with the dissociation of NGH. According to triaxial experiments (Lu et al., 2008): "The strength after dissociation of hydrate is about 1/7 of that before dissociation when the hydrate with the skeleton of Mongolia sand. The strength after dissociation of hydrate is about 3/5 of that before dissociation when the hydrate with the skeleton of clay brick, while the cohesion after dissociation of hydrate is about 1/3 of that before dissociation." Therefore, the strength at these areas with higher pore pressure is lower, which causes the soils move from the upper part to the toe and meanwhile settle gradually. Generally the following equation (1) can be used as the criterion to judge the instability of soils at any point in the slope. In this way a sliding surface can be obtained, above which, the part is instability.

$$\tau_f < F \tag{1}$$

in which $F = \rho g h \sin\theta$, θ is the slope angle.

3 CONCLUSIONS

Main conclusions are as follows:

1. The centrifugal experiment, which can model the effects of the gravity acceleration, is an effective method to investigate the seabed instability induced by gas hydrate dissociation because it can.
2. The gas produced after NGH dissociation can cause the increase of pore pressure and the decrease of effective stress. The slope tends to slide towards the toe which insults that the slope angle becomes smaller.
3. The failure occurs first at the toe of the slop and slides downwards along an arc sliding face. Cracks form at the top of the slope.
4. The pore pressure at the upper part and near the sidewall increase faster than that at the rest part with the dissociation of GH.
5. If HBS is locally heated, gas hydrate dissociates faster near the heater and the pore pressure is larger than that under room temperature.
6. If there is an over layer with low permeability or is dissociated faster (such as by heating), the settlement and pore pressure become larger than that without such a cover layer and dissociating slowly.

ACKNOWLEDGMENT

This paper is supported by the National Science Foundation (No. 11102209; No. 11272314).

REFERENCES

Gilles, G., David, G., and Aaleksandr, M. 1999. Characterization of in situ elastic properties of NGH-bearing sediments on the Blake Ridge," *J Geophysical Research*, 104(B8): 17781–17795.

Hovland, M., Orange, D., Bjorkum, P.A. et al. 2001. NGH and seeps-effects on slope stability," *Proc. 11th Int. Offshore and Polar Engrg. Conf.,* 11: 471–476.

Kayer, R.E., and Lee, H. 1991. Pleistocene slope instability of NGH-laden sediment on the Beaufort Sea Margin," *J Marine Geotechnology*, 10(1–2): 125–141.

Locat, J., and Lee, H.J. 2002. Submarine landslide, advances and challenges, *J Canada Geotechnology*, 39: 93–212.

Lu X.B., Wang L., Wang S.Y. et al. 2008. Study on the mechanical properties of THF hydrate deposit. *Proc. 18th Int. Offshore and Polar Engrg. Conf.*, Vancouver, 57–60.

Lu X.B., Wang L., Wang S.Y. et al. 2010. Instability of seabed and pipes induced by NGH dissociation, *Proc.20th Int. Offshore and Polar Engrg. Conf.*, Beijing, 110–114.

Lu X.B., Zhang X.H., Wang S.Y. 2011. Strong failure of seabed induced by gas hydrate dissociation, *7th Int. Conf. Gas Hydrate*, Edinburgh.

Masui A., Haneda H., Ogata Y. et al. 2005. Effect of methane hydrate formation on shear strength of synthetic methane hydrate sediment. *Proc. 15th Int. Offshore and Polar Eng. Conf.,* Seoul, Korea, 364~369.

Sakamoto Y., Komai T., Kawamura T. et al. 2007. Field scale simulation for the effect of relative permeability on dissociation and gas production behavior during depressurization process of methane hydrate in

marine sediments. *Proc. ISOPE Ocean Mining Symp.,* Lisben, Portugal,102–107.
Sakamoto Y., Kakumoto M., Miyazaki K. et al. 2009. Numerical study on dissociation of methane hydrate and gas production behavior in laboratory-scale experiments for depressurization: Pat-3-numerical study on estimation of permeability in methane hydrate reservoir. *Int. J. Offshore and Polar Engrg.,* 19(2): 124–134
Sultan, N., Cochonat, P., Foucher, J.P. et al. 2004. Effect of NGHs melting on seafloor slope instability," *J Marine Geology*, 213: 379–401.
William, J.W., Ingo, A.P., William, F.W. et al. 2004. Physical properties and rock physics models of sediment containing natural and laboratory-formed methane NGH," *J American Mineralogist,* 89: 1221–1227.
Zhang X.H., Lu X.B., and Zheng Z.M. 2011. Layered fracture and outburst due to dissociation of hydrate, *J. Petroleum Science and Engrg.,* 76: 212–216.